

High-Precision Adaptive Control of Large Reflector Surface

H. Fang, E. Im and U. O. Quijano

Jet Propulsion Laboratory, California Institute of Technology
4800 Oak Grove Drive
Pasadena, CA 91109 USA

K. W. Wang and J. Hill

Department of Mechanical and Nuclear Engineering, The Pennsylvania State University
157 Hammond Bldg.
University Park, PA 16802 USA

J. Moore and Jim Pearson

ManTech SRS Technologies
500 Discovery Drive
Huntsville, AL 35806 USA

C. Lui and F. Djuth

Geospace Research, Inc.
525 Douglas Street
El Segundo, CA 90245 USA

Abstract—An innovative high-precision adaptive control architecture for large membrane and thin-shell reflectors is presented. The associated component technologies which include the inflatable membrane reflector, PVDF actuator and the analytical model are also discussed by this paper.

I. INTRODUCTION

Under NASA's Earth Science Technology Program, a novel high-precision adaptive control architecture and the associated component technologies is being developed for large antenna reflectors. A large and high-precision reflector implies high RF frequency and high resolution, which is greatly demanded by earth science mission planners and gives them the flexibility in choosing of orbits such as LEO, MEO and GEO. It can be employed by radar and radiometer to monitor resources, weather and to perform hazard assessment [1]. Due to the large size (from several meters to several tens of meters), the reflector needs to be an in-space deployable and light-weight to accommodate the fairing size and weight requirements of the launch vehicle. However, how to maintain the surface figure accuracy of a large deployable reflector is extremely challenging.

Fig. 1 shows the architecture of the high-precision surface control system. It consists of a large deployable reflector, a set of flexible actuators (mounted on the back of the reflector), a wavefront sensing metrology subsystem, and an active (feedback) controller. The metrology subsystem periodically measures the surface contour and sends the information to the controller. Guided by shape control laws, the controller updates voltage signals to

control the actuator strain at various positions to maintain the desired shape contour. This paper will discuss the component technologies of this architecture which include the inflatable membrane reflector, flexible PVDF film actuator, and analytical modeling of the system.

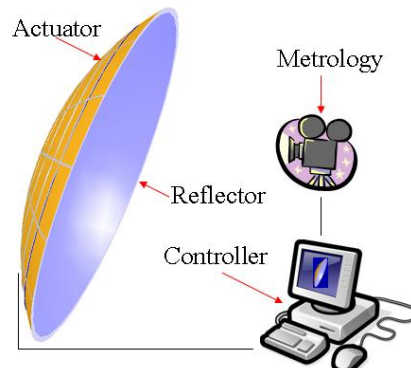


Fig. 1. Architecture of the high-precision adaptive control system

II. INFLATABLE MEMBRANE REFLECTOR

This study uses an inflatable membrane reflector as the test article to investigate the high-precision adaptive control technology. Besides inflatable membrane reflectors, this technology can also be employed to other thin shell reflectors. A typical inflatable reflector consists of two thin films, a reflector and a canopy, that are joined around the edges. The relatively thin (several tens of micro-meters) polymer films are cast on a precisely shaped mandrel and then thermally cured and released. The reflector film is typically metalized with a vapor deposited silver or

aluminum coating, nominally 1200 Å thick. The membranes are then joined using a leak tight bonding technique. Following fabrication, the reflector is integrated with an inflatable torus or radome via compliant features that minimize loading changes associated with thermal excursions. Fig. 2 shows two such inflated reflectors. The reflector and torus structures are precisely inflated to approximately achieve the desired membrane stress and structural stiffness. Then, the boundary tension is adjusted to achieve the best shape. While the reflector film and canopy film are cast as one piece polymer thin films with a parabolic shape, achieving high surface accuracy after inflation deployment and in the space thermal environment is more challenging. Inflation pressure and film stress introduce shape errors, especially slope error near the edges (characteristic Hencky (W Error)). Thermal loads cause less systematic shape errors. The thermal induced shape errors can be significant and may drive the need for active control of the inflatable reflector. However, recent improvements in low coefficient of thermal expansion space ratable polymers can potential reduce the magnitude of thermal distortions [2].



Fig. 2. 10- and 5-meter inflatable reflector

NASA and ManTech SRS Technologies have successfully collaborated on research and development of lightweight thin-film reflectors. To date, on-axis, off-set, and Cassegrain antennas, from 0.3m to 4m in aperture, have been designed, fabricated, and radio frequency (RF)

characterized via range testing [3]. The designs address requirements for space based systems as well as inflatable terrestrial radome reflectors. Fixed, deployable, and adaptive test structures are being developed to support the thin film reflectors during testing and future operations. RF characterizations of off-set and on-axis reflectors have been performed in the NASA GRC Far Field and Near Field facilities at frequencies from X-band to Ka-band. Thus far, frequencies through Ku-band have indicated excellent RF performance. Ka-band test results indicate that improved reflector surface shape accuracy (sub-millimeter values) is required for efficient operation. Thus, shape optimization, tooling technology, fabrication processes, and active shape control techniques are being considered to enable Ka-band operations.

All of this successful lightweight inflatable thin-film reflector research and development has the potential to enhance current RF capabilities and enable many future RF requirements that need efficiently packaged deployable reflectors with large apertures. Fig. 3 shows RF characterization data from the 4-m x 6-m testing. This data demonstrates the X-band reflector performance while showing the need for shape improvement to extend performance to Ka-band

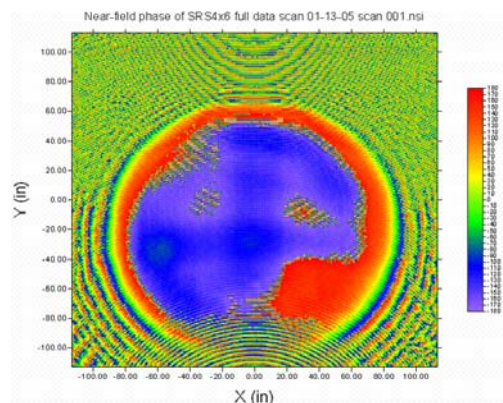
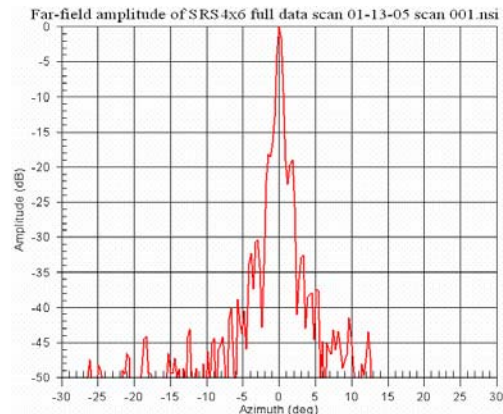


Fig. 3. 8.4 GHz data for 4-m x 6-m test article

There are a number of technical challenges for large inflatable thin film reflectors. The primary challenge is shape errors reduction to enable Ka-band and other higher frequency applications. The shape errors are the result of inflation pressure (membrane effects including Hencky W-error, oil can, other boundary errors) and thermal distortions. Key technologies being developed to address the challenges include: 1) improved membrane materials, 2) active control and 3) improved tooling and manufacturing processes.

Thermally induced shape aberrations are also significant. Resulting shape errors can be large (for example, 13.9 mm for a 35-meter polyimide reflector in geosynchronous orbit) [4]. Static shape optimization alone is not an option for inflatable reflector made from the current generation of space rated polymer materials under most operational scenarios. Possible solutions include low or zero CTE membrane materials and / or active shape control. As shown in Fig. 4, reduced CTE materials can help enable very large ultra-light deployable apertures for high band width communications, space science, earth science, and other applications.

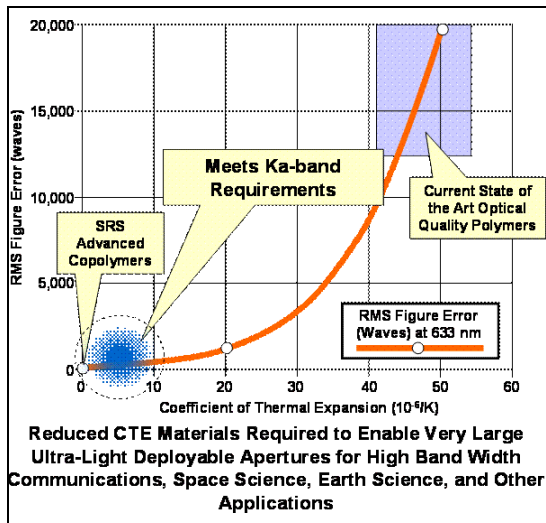


Fig. 4. Low CTE Data

Together with all aforementioned being developed technologies, the high-precision adaptive control technology developed by this study will ultimately enable the large inflatable membrane reflector to be used for Ka-band and/or even higher RF frequencies.

III. PVDF ACTUATOR FABRICATION

Since an inflatable membrane reflector is composed of very thin materials, the actuator has to be very thin (several

tens of micro-meters) and very flexible. Currently available PZT based actuators are not applicable for this application. An innovative actuator technology, namely flexible PVDF film actuator technology, is being developed by this study. This technology is extremely suitable and highly effective in controlling the surface precision for large, extra lightweight thin-material antenna reflectors. Besides RF applications, this technology is also readily applicable to optical applications such as nano-laminate mirrors and thin film mirrors.

A fabrication process has been developed for the PVDF actuators [5]. In general, the fabrication process consists of film preparation, stretching, poling and electrode deposition (Fig. 5). PVDF thin films are prepared by either casting polymer solution on substrates or pressing polymer melts using heated plates. The films are then stretched to several times along one direction. Poling can be done by contact poling where electric field is directly applied across the film through two contact electrodes. Corona poling is an alternative poling method [6]. In corona poling, film has electrode on only one side and a sharp needle is placed at a certain distance away from the other side. When very high voltage is applied between the needle and the bottom electrode, air ionization happens around the needle and the generated charges accumulate on the film surface, establishing a poling electric field in the film. The poled films are coated with metal or conducting polymer electrodes. Metal electrodes such as silver and gold are deposited by sputtering or thermal evaporation, while conducting polymers can be deposited by screen printing. Compared to the vacuum deposition systems required for metal electrodes, screen printing equipments are much less expensive and can be easily scaled up, and hence the conducting polymer is especially attractive as electrodes for large scale films.

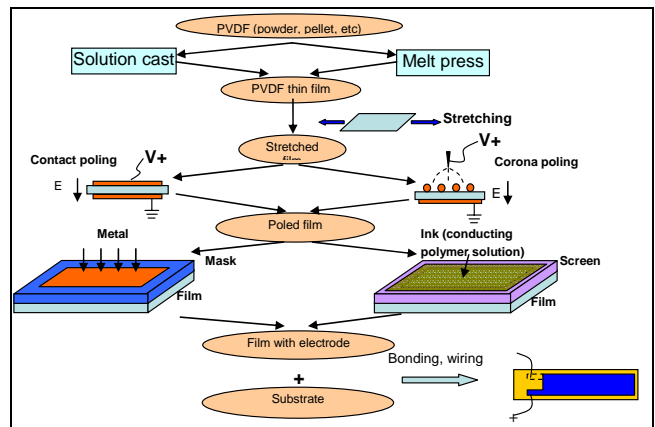


Fig. 5. PVDF actuator fabrication process

IV. MODELING

A. Reflector Modeling

The reflector is modeled as a thin shallow spherical cap [7], while assuming pre-stress due to the internal inflation pressure. Simply supported boundary conditions at the rim are also assumed. The displacement (u , v , and w) are defined relative to a spherical coordinate system, seen in Fig. 6, which coincides with the lines of principal curvature of the mid-surface.

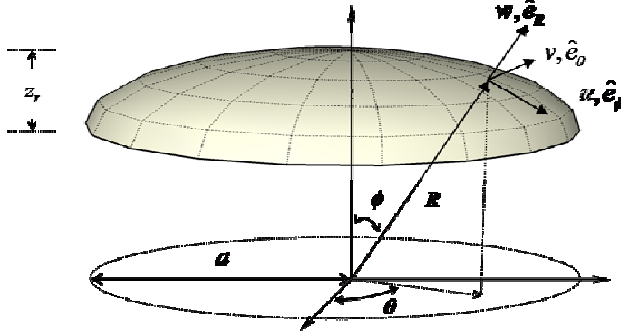


Fig. 6. Coordinate system for reflector model

Because the reflector is very thin, the Love simplification can be used, which is that the displacements u and v are assumed to vary linearly with the shell thickness, while displacement w can be assumed to not vary with the shell thickness.

Using these simplifications, the total reflector strain energy can be calculated, which includes the elastic strain energy, the strain “growth” due to the thermal expansion, along with additional strain energy caused by the inflation of the reflector. The total energy for the actuator can be formulated using the appropriate constitutive equation and the strain-displacement relationship of the actuator. The entire surface of the reflector can be covered with actuators, or single actuators can be placed at will on the surface.

To derive the system equations from the total strain energy formulation, the Ritz method utilizing a Fourier-Bessel series expansion is used. These expansions satisfy the boundary condition.

The modeling of the reflector incorporates the effect of the actuators on the surface displacement, along with the effect of the temperature profile on the reflector. The temperature profile is assumed to be a combination of a uniform temperature change (the entire surface changes the same amount), which we will call T_0 , and a linear temperature gradient over the surface, which would be caused from the sun shining at an oblique angle on the reflector, ΔT .

As the model was refined, several time-dependent phenomena were added. Diurnal changes to the temperature

gradient across the reflector are included, which allows a day-in-the-life type of simulation of the required adjustments of the actuators and of the reflector’s consequent surface quality. The model also includes the reflector’s vibratory response to sudden commanded changes to the actuators.

B. Control Algorithm

Due to the quasi-static nature of the reflector system, a Least Squares (LS) controller has been used. The input for the LS controller is the displacement at all metrology points. Using the matrix form from the linear equations from the model, the desired actuation voltages x can be found by minimizing (1),

$$\frac{1}{2} \|Cx - e\|_2^2 \quad (1)$$

where e is the displacement error at the metrology sensor points and C is the matrix formed from the model matrix. Once the controller determines the actuation voltages, they are applied to each actuator, and the total displacement is calculated.

C. Influence Coefficient Matrix

The model together with the control algorithm described in Sections (A) and (B) are used to evaluate the system performance for preliminary studies and design guideline formulation. However, to ensure that the system will perform well even when analytical models are not accurate or not available, an “Influence Coefficient Matrix” (ICM) approach has been devised. In this approach, the response of a physical reflector’s entire surface to changes in each actuator is measured, and by analyzing this information the controller can determine the actuator voltages needed to correct the surface figure in the desired way. Since this method does not require an analytical model, the imperfections and idiosyncrasies of a given reflector can be captured by this approach. Measurement uncertainty and random errors can be reduced by taking multiple measurements for each actuator and averaging them.

D. Results

Results are given for a fully covered, 35-meter diameter reflector. The material and geometric values used are shown in Table I.

TABLE I
MATERIAL AND GEOMETRIC VALUES

	Reflector	PVDF
Density	$\rho = 1420 \text{ kg/m}^3$	$\rho = 1780 \text{ kg/m}^3$
Elastic Modulus	$E_{\text{Young's}} = 2.5 \text{ GPa}$	$E_{\text{Young's}} = 2.27 \text{ GPa}$
Poisson’s Ratio	$\nu = 0.225$	$\nu = 0.225$
Coefficient of Thermal	$a_{CTE} = 20 \times 10^{-6} \text{ K}^{-1}$	

Expansion		
Yield Stress	$\sigma_y = 172 \text{ MPa}$	
Piezoelectric Constants		$d_{31} = 15 \times 10^{-12} \text{ m/V}$ $d_{32} = 4 \times 10^{-12} \text{ m/V}$
Coercive Field Strength		$E_{\text{pol}} = 80 \text{ MV/m}$
Maximum allowed voltage		$VE_{\text{max}} = 1620 \text{ V}$
Radius of Curvature	$R = 56 \text{ m}$	
Planform Radius	$a = 17.5 \text{ m}$	
Center Rise Height	$z_r = 2.805 \text{ m}$	
Thickness	$h_{\text{ref}} = 50 \text{ }\mu\text{m}$	$h_{\text{act}} = 50 \text{ }\mu\text{m}$

Two sets of results are given: the surface error from the uniform temperature shift, T_0 , and the surface error from the gradient temperature shift, ΔT . Fig. 7 and Fig. 8 show the surface error with respect to the temperature shift. The black line signifies the surface error without any control, while the gray line is the surface error after control.

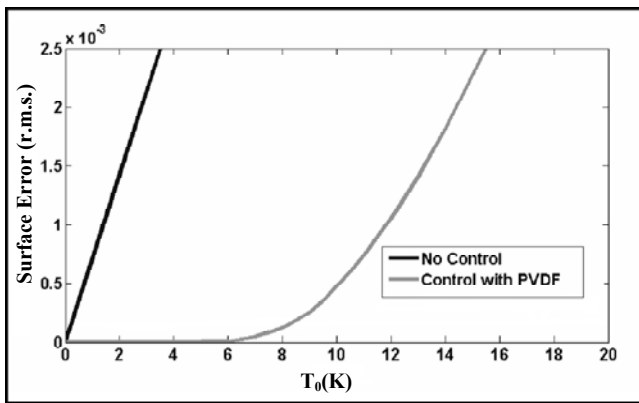


Fig. 7. Surface error as a function of ΔT

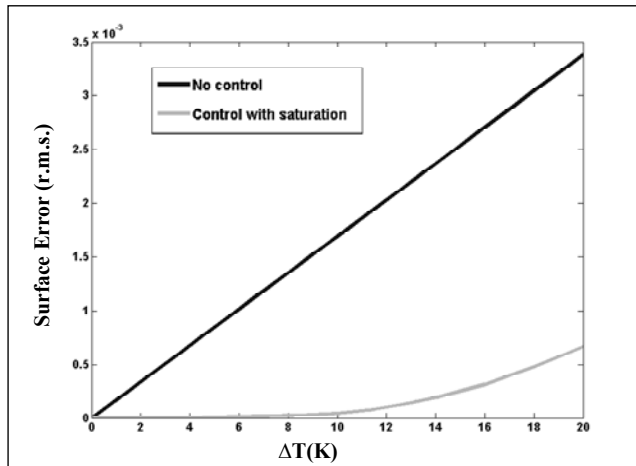


Fig. 8. Surface error as a function of ΔT

As the temperature of the reflector increases, the surface error increases dramatically. The reflector with treatment and control has a much lower surface error. As the actuators become saturated, the surface error can not be

fully controlled, but still is considerably better than the non-controlled surface.

V. ENGINEERING MODELS

In order to demonstrate the feasibility of this innovative reflector surface figure control technology, a 0.2-meter diameter membrane reflector engineering model has been assembled and tested [5]. The PVDF films used for this model were obtained from KTech Company and were corona poled. In order to increase the actuation authority, double layer actuators ($2 \times 25 \mu\text{m}$) have been fabricated, where the poling direction of the two films were aligned to the same direction and the electrodes were connected so that opposite electric fields were applied on the two films. To implement the PVDF films on the thin-membrane reflector, a mold has been designed and fabricated for attaching actuators to the reflector. The deformation of reflector under applied electric field was measured using a test system which includes the laser metrology unit, digital readout, the power supply, and the test reflector (Fig. 10).

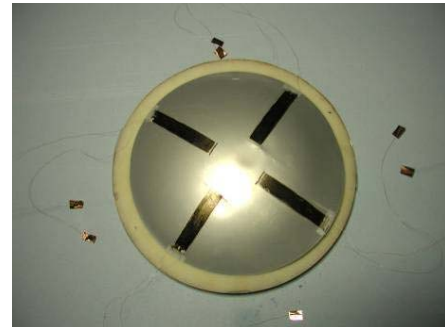


Fig. 9. The 0.2-m diameter engineering model. The reflector (silver) was placed on the mold (white).

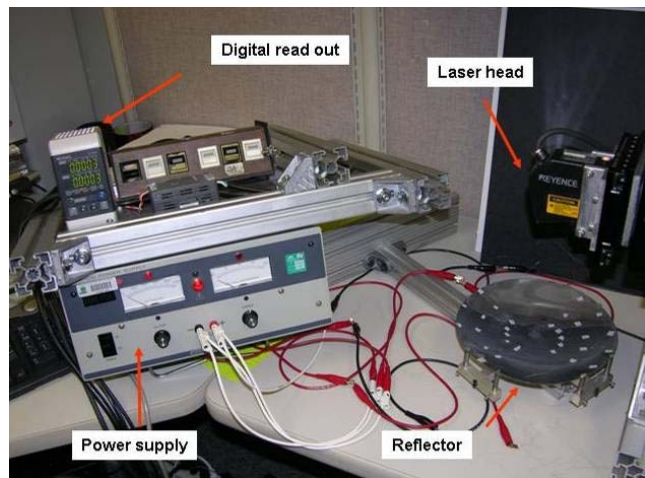


Fig. 10. Test set up for measuring the reflector deformation

The test results showed that the PVDF actuators as developed appear to achieve the required actuations. A 2.4-m diameter inflatable membrane reflector as well as the associated PVDF actuators is being fabricated by this study to quantitatively investigate the functionality of the high-precision adaptive control technology.

VI. CONCLUSIONS

An innovative high-precision adaptive control architecture for large membrane and thin-shell reflectors is being developed. The inflatable membrane reflector, PVDF actuator and the analytical model are discussed by this paper. A 0.2-m diameter breadboard has been fabricated to demonstrate the feasibility of this adaptive control technology. A 2.4-m diameter breadboard is being fabricated to quantitatively investigate the functionality of this technology.

ACKNOWLEDGMENTS

Authors would like to express the appreciations to Qin Chen, Don Natale, Bret Neese, Kailiang Ren, Minren Lin, and Q. M. Zhang of PSU for their help and support. The work described is performed at Jet Propulsion Laboratory, California Institute of Technology, Pennsylvania State University, ManTech SRS Technologies, and Geospace Research, Inc. under a contract with the National Aeronautics and Space Administration.

REFERENCES

- [1] E. Im, M. Thomson, H. Fang, J.C. Pearson, J. Moore, J.K. Lin, "Prospects of Large Deployable Reflector Antennas for a New Generation of Geostationary Doppler Weather Radar Satellites," AIAA-2007-9917, AIAA SPACE 2007 Conference & Exposition, Long Beach, California, September 18-20, 2007
- [2] G. Poe, "Heteropolymeric Polyimide Polymer Compositions" PCT Pat. App. No. PCT/US06-29805.
- [3] James C. Pearson, Dr. Robert Romanofsky, "Thin Film Antenna Development and Optimization", 14th AIAA/ASME/AHS Adaptive Structures Conference, Newport, Rhode Island, 1-2 May 2006
- [4] S. Chodimella, J. Moore and J. Otto, H. Fang, "Design Evaluation of a Large Aperture Deployable Antenna", AIAA-2006-1603 47th AIAA/ASME/ASCE/AHS/ASC Structures, Structural Dynamics, and Materials Conference, Newport, Rhode Island, May 1-4, 2006
- [5] Q. Chen, D. Natale, B. Neese, K. Ren, M. Lin, Q. M. Zhang, M. Pattom, K. W. Wang, H. Fang, and E. Im, "Piezoelectric Polymers Actuators for Precise Shape Control of Large Scale Space Antennas", SPIE Smart Structures and Materials & Nondestructive Evaluation and Health Monitoring 14th International Symposium, San Diego, California, March 18-22, 2007
- [6] T. Kaura, R. Nath, and M. M. Perlman, "Simultaneous stretching and corona poling of PVDF films", *J. Phys. D.*, 1848-1852 (1991)
- [7] W. Soedel, *Vibrations of shells and plates*, 3rd ed. New York: , 1993.